

THE VELOCITY AND TEMPERATURE FIELDS OF RECTANGULAR JETS

A. A. SFEIR

Mechanical Engineering Department, American University of Beirut, Beirut, Lebanon

(Received 25 August 1974 and in revised form 6 July 1975)

Abstract—The mean velocity and temperature profiles of rectangular jets having different aspect ratios and nozzle geometries were measured using hot-wire anemometry. The temperature excess in the jet was small so that temperature could be treated as a passive scalar. The flow-field, for both velocity and temperature, is found to be divided in three distinct regions respectively referred to as, the potential core, the two-dimensional region and the axisymmetric region. These regions are not the same for the velocity and temperature distributions. The extent of each of these regions is a function of the nozzle aspect ratio. The flow in the two-dimensional region as well as the transition to axisymmetry are strong functions of the nozzle geometry. At large distances from the nozzle exit, both the velocity and temperature fields are found to behave in the same way as in the flow out of a circular nozzle of the same area.

NOMENCLATURE

d , jet width in the y direction;
 d_0 , nozzle slit width;
 d_T , jet width with respect to temperature distribution in the y direction;
 l , jet width in the z direction;
 l_0 , nozzle slit length;
 l_T , jet width with respect to temperature distribution in the z direction;
 n , empirical coefficient in the velocity-decay equation;
 t , temperature fluctuation;
 u , fluctuation of the velocity along the x axis;
 v , fluctuation of the velocity along the y axis;
 x , distance from jet exit measured parallel to jet axis;
 \bar{x} , nondimensional distance along x ;
 y , distance along the slit height;
 z , distance along the slit length;
 A , nozzle aspect ratio;
 A_e , equivalent jet momentum area;
 A_{eT} , equivalent jet heat flux area;
 C_1, C_2 , jet virtual origin;
 D_1, D_2 , jet virtual origin;
 K_1, K_2 , empirical constants of the centerline velocity and temperature decay in the two-dimensional region of the jet;
 L_1, L_2 , empirical constants of the centerline velocity and temperature decay in the axisymmetric region of the jet;
 Re_{d_0} , Reynolds number based on d_0 ;
 T , mean temperature;
 T_c , mean temperature along the centerline;
 T_j , mean temperature at the nozzle exit;
 \bar{T} , nondimensional mean temperature;
 U , mean velocity in the x direction;
 U_c , mean velocity along the centerline;
 U_j , mean velocity at the jet exit;
 \bar{U} , nondimensional mean velocity;
 V , mean velocity in the y direction.

Greek symbols

η , nondimensional distance along y ;
 θ , jet momentum thickness;
 θ_T , jet heat flux thickness;
 ξ , nondimensional distance along z .

1. INTRODUCTION

TURBULENT jets have been the subject of many theoretical and experimental investigations; their important role in the many aspects of engineering has recently given a new impetus for more detailed studies of these flows.

Until recently very limited attention has been given to the jet out of a rectangular nozzle and its subsequent transition to axisymmetry. To our knowledge, the only published information on this aspect of turbulent free jets is the work done at the Polytechnic Institute of Brooklyn by Sforza *et al.* [1], Trentacoste and Sforza [2] and Sforza [3]. These experimental and theoretical investigations have shown that the flow field of the incompressible jet out of a rectangular nozzle may be subdivided into three main regions: the potential core region or region of jet flow establishment where the centerline velocity $U_c = \text{constant}$, followed by the two-dimensional region where $(U_c)^2 \propto x^{-n}$ with $n \approx 1$, and then a region extending to infinity where the centerline velocity decay is characteristic of axisymmetric jets, i.e. $U_c \propto x^{-1}$. The extent of each of these regions has been shown to be a function of the nozzle aspect ratio. The exponent n is also a function of the aspect ratio according to the above mentioned studies.

As far as concentration measurements are concerned, the most complete study known to us is that of Van Der Hegge Zijnen [4] which is however limited to the two-dimensional zone of the jet. In this study temperature measurements and concentration measurements are compared, and it is deduced that the diffusion of heat is similar to that of mass. Van Der Hegge Zijnen [4] compares his temperature (or concentration) measurements to the different theories of heat transfer across

plane jets and finds a substantial lack of agreement with all these theories.

Many other investigations dealing with the two-dimensional region of the jet, and measuring mean velocity and turbulence have also appeared; of the most recent and more detailed ones are the work of Bradbury [5] and Heskestad [6]. In general however, appreciable lack of agreement in the centerline velocity decay and jet spread may be noted between most of the published results. A better agreement is obtained when comparing the velocity profiles across the jet, which, in most cases is well represented by a gaussian distribution.

In the present investigation, the flow fields of jets of different aspect ratios and two types of nozzle geometries are studied. The mean velocity field and mean concentration, simulated with a temperature excess, were measured using hot wire anemometry. The initial temperature excess was of the order of 60°F, which made buoyancy effects rather negligible. The Reynolds number based on the slit height, was for all the experiments: $Re_{d_0} = 122\,200$; the three aspect ratios tested were respectively 10, 20 and 30.

The three regions of the jet flow field for both velocity and temperature are studied in terms of the effects of nozzle geometry and aspect ratios. It is found that the flow in the two-dimensional zone is practically independent of the nozzle aspect ratio, a result which contradicts the results of [2]. The nozzle geometry on the other hand, was found to have an important effect on the flow in the two-dimensional region and on the transition from two-dimensional to axisymmetric flow. The three main regions of the flow are also determined in terms of the centerline temperature decay. It is found that, as the diffusion of mass and heat is faster than that of momentum. The two-dimensional region as far as T is concerned, starts at a smaller distance from the nozzle than the two-dimensional region determined from the velocity field; the same is also true for the axisymmetric region. At large distances from the nozzle exit, the centerline velocity and temperature decays are found to behave in the same way as in the flow out of a circular nozzle of the same area.

2. EXPERIMENTAL APPARATUS AND TECHNIQUES

The experiments described herein were performed in the Mechanical Engineering Laboratories of the School of Engineering and Architecture at the American University of Beirut.

Two types of nozzles were tested. Nozzles referred to as type I consisted of rectangular slots with sharp edges. Nozzles of type II consisted of rectangular channels of length equal to fifty slot heights. Slot length, height, and aspect ratio are referred to respectively by l_0 , d_0 and $A = l_0/d_0$.

The flow facility consisted of using a low-speed wind-tunnel that was built as a prototype of a large scale one currently under construction. This facility is described by Bassam El As'ad [7]. The 6×6 in test section was removed and replaced by a specially built section with heater elements, which could be fitted at its exhaust by nozzles with $d_0 = 4$ mm and aspect ratios

up to 30. This section had a total length of 50 in and it had attached at its upstream end eight electric heater elements followed by two fine mesh screens 6 in downstream. Between the two screens a mercury thermometer with an electric contact was placed and connected to an electronic relay switch which turned on and off three of the heater elements at a given adjustable temperature level. This arrangement yielded a jet velocity U_j varying not more than 1% over the duration of each experiment. The temperature was adjusted at $146 \pm 2^\circ\text{F}$ for all the experiments; in each experiment T was found to vary less than $\pm 1^\circ\text{F}$ provided the apparatus was left to warm up for around half an hour. Velocity measurements were obtained using a hot-wire anemometer and a total-head probe connected to a Hewlett-Packard model 290 pressure transducer. Good agreement between the two measuring techniques was usually obtained. Most of the data presented here were obtained with the aid of the not-wire probes operated with a Thermo-systems Inc. Model 1050 constant temperature anemometer set. A fourth-order Polynomial Linearizer Model 1052 and a Signal Conditioner Model 1057 of the same make were also used. The temperature measurements were performed using the same hot wire set but operating the sensor as a linearized resistance thermometer.

The hot-wire probes were held along the jet axis at the end of a 12 in-long probe holder. This was attached to a traversing mechanism operated manually and capable of motion along the three axes. The probe location was monitored with Hewlett-Packard displacement transducers. This arrangement allowed for direct plotting of velocity and temperature levels versus position on an x - y recorder of the same make.

Hot-wire probes were made of 0.00015 in tungsten wire, the wire lengths being approximately equal to 0.0625 in. These were calibrated before and after each run and usually it was found that both calibrations were identical. However, over long time lapses, a noticeable drift occurred and the linearizer's polynomial constants were readjusted to account for it.

3. THEORETICAL CONSIDERATIONS

The fundamental equations of motion and heat transfer for a two-dimensional jet are:

$$U \frac{\partial V}{\partial x} + V \frac{\partial V}{\partial y} = \frac{\partial}{\partial y} (\bar{u}v) \quad (1)$$

and

$$U \frac{\partial T}{\partial x} + V \frac{\partial T}{\partial y} = \frac{\partial}{\partial y} (\bar{u}T) \quad (2)$$

and the equation of continuity:

$$\frac{\partial U}{\partial x} + \frac{\partial V}{\partial y} = 0. \quad (3)$$

Equations (1) and (2) are valid only for boundary layer type flows in which the temperature difference is sufficiently small so that buoyancy effects remain negligible. In the case of small temperature differences, the temperature field is known to behave similarly to any passive scalar field.

Writing

$$U = U_c f(\eta)$$

and

$$T = T_c g(\eta)$$

where U_c and T_c are the values of the mean velocity and mean temperature along the centerline and $\eta = (y/x)$, the usual assumptions of self-preservation yield:

$$\begin{aligned} U_c &\propto x^n \\ T_c &\propto x^n \\ d &\propto x \\ d_T &\propto x \end{aligned} \tag{4}$$

where d is the jet half-width (distance from the centerline to the point where $U = (U_c/2)$) and d_T is a similarly defined jet half-width with respect to the temperature distribution.

Integrating equations (1) and (2) across the jet we get the equations of conservation of momentum and heat flux which may be written:

$$\begin{aligned} \int_{-\infty}^{+\infty} U^2 dy &= \text{const} \\ \int_{-\infty}^{+\infty} TU dy &= \text{const}. \end{aligned} \tag{5}$$

These quantities are respectively equal to the momentum flux and the thermal flux at the mouth of the jet. Equations (4) and (5) yield:

$$\begin{aligned} \left(\frac{U_c}{U_j}\right)^2 &= K_1(\bar{x} - C_1)^{-1} \\ \left(\frac{T_c}{T_j}\right)^2 &= K_2(\bar{x} - C_2)^{-1} \end{aligned} \tag{6}$$

where \bar{x} is the nondimensional distance from the jet exit.

A similar analysis yields for the axisymmetric jet:

$$\begin{aligned} \frac{U_c}{U_j} &= L_1(\bar{x} - D_1)^{-1} \\ \frac{T_c}{T_j} &= L_2(\bar{x} - D_2)^{-1}. \end{aligned} \tag{7}$$

Equations (6) and (7) will be compared to our experimental results in the next section.

4. EXPERIMENTAL RESULTS

4.1. The mean velocity field

Measurements of the mean velocity field are expressed in terms of the centerline velocity decay, the jet width and the velocity profiles in the y and z directions across the jet. The x axis is taken along the centerline of the jet with origin at the jet outlet, and y and z directions are taken along the slit height and length respectively.

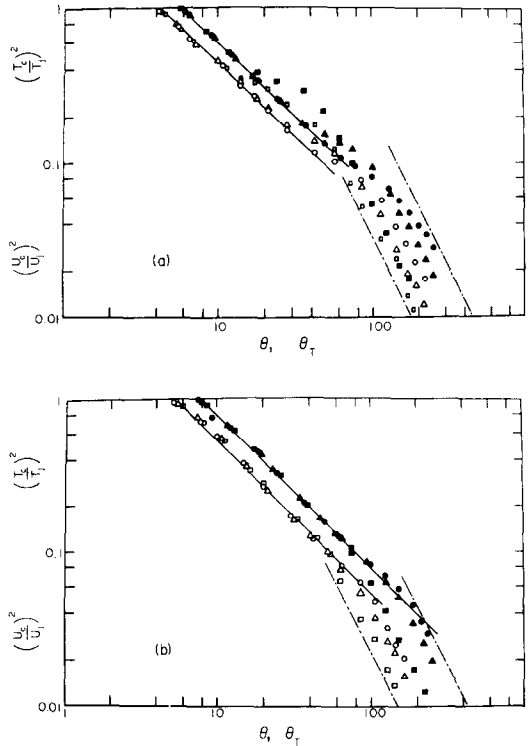


FIG. 1. Centerline velocity and temperatures; (a) nozzle type I; (b) nozzle type II. \square and \blacksquare , T_c and U_c respectively for $A = 10$; \triangle and \blacktriangle for $A = 20$; \circ and \bullet for $A = 30$.

Centerline velocity decay. Figure 1 shows measured values of $(U_c/U_j)^2$ at different stations downstream of the jet exit. In this figure the distance x is non-dimensionalized by dividing it by the jet momentum thickness:

$$\theta = \int_{-\infty}^{+\infty} \left(\frac{U}{U_j}\right)^2 dy.$$

This parameter is preferable to the nozzle height d_0 ; it is equal to it if one has a uniform velocity distribution at the nozzle exit which is not the case with either type of nozzle geometry tested. The parameter θ was deduced from velocity profiles taken at different stations downstream of the jet exit. In the case of the flow out of the sharp edged nozzle, θ increases slightly with the distance from the nozzle exit and reaches a constant value at $(x/d_0) > 1.5$. This is due to the pressure variation which is present in the flow field through a sharp orifice.

Our results are qualitatively very similar to those of Trentacoste and Sforza [2] and one can distinguish the region of flow establishment or potential core where $(U_c/U_j) = 1$, followed by the two-dimensional region where $(U_c/U_j)^2 \propto (\theta/x)$, then a final region extending presumably to infinity, where $(U_c/U_j) \propto (\theta/x)$. The extent of each of these regions as well as the transition between one and the next are difficult to pinpoint accurately. The length of the two-dimensional zone as well as that of the transition zone to axisymmetric flow are quite different for the two nozzle geometries tested. Figure 1(a) shows that the flow out of the nozzle with

sharp edges and $A = 20$ is nearly two-dimensional up to $(x/\theta) \approx 40$, while for the flow out of the channel this figure becomes $(x/\theta) \approx 100$. Also, while the slope changes monotonically from -1 to -2 in Fig. 1(b), it is not so for the other case. This difference is associated with the mechanism of transition which will be discussed later. A slight difference can also be noted at the beginning of the two-dimensional region where, in the flow out of the sharp nozzle, the slope of $(U_c/U_j)^2$ tends to -1 from larger values while the opposite is true for the other nozzle. This indicates that the jet virtual origin C , has different signs for the two nozzle geometries tested.

The centerline velocity decay constants obtained by fitting equation (6) to the experimental points are shown in Table I along with some previously published results

data points in the axisymmetric region will fit a relation as in (7) and where the constants L_1 are practically independent of A . Values of the constants L_1 obtained are shown in Table 1. The scatter between these values is rather small and may well be due to the fact that few experimental points are used in determining L_1 in all but the smallest aspect ratios. Comparing our results with those of Trentacoste and Sforza [2], it seems reasonable to conclude that equation (7) does represent satisfactorily the centerline velocity decay in the axisymmetric region of the two-dimensional jet. Comparing our results with measurements in circular jets, we can also conclude that at large distances from a jet out of a rectangular slit, the centerline velocity decay is nearly similar to that of a circular jet of the same orifice area.

Table I. Centerline velocity decay constants

Investigators	2-D region		Axisymmetric region						Circular jet	
	K_1	K_2	$A = 10$		$A = 20$		$A = 30$		L_1	L_2
Albertson <i>et al.</i> [10]										6.25
Bradbury* [5]	6.25									
Forstall and Gaylord [11]									6.4	5.2
Heskestad [6]	2.75									
Hinze and van der Hegge Zijnen [12]										6.25
Sforza <i>et al.</i> [1]	5.3-7.8		7.0		5.64					
Van der Hegge Zijnen [4]	4.9-6.15	4								
Present data*										
Nozzle type I	6.4 ± 0.2	4.58	6.19	4.69	6.10	4.19	6.21	4.18		
Nozzle type II	7.3 ± 0.2	5.35	6.25	4.64	6.0	4.2	5.8	4.07		

*For the data reported by Bradbury as well as the present results, x is nondimensionalized using the jet momentum thickness θ instead of the jet thickness d_0 .

on two-dimensional jets. These constants are independent of the aspect ratio but are different for the two nozzles tested. This discrepancy is partly due to the fact that the nozzles with sharp edges were machined flat in plates of dimensions at least equal to $20 d_0$ all round the slot, while the channels were made to protrude into the ambient air surroundings. By placing flat plates normal to the channel at exit it was noted that for $A = 20$ the value of K_1 dropped by 6%. This effect does not however explain all the difference in the values of K_1 as will be seen later. The results of [2] show a large dependence of K_1 on A , but it must be pointed out that the conditions of the experiments are not similar; whereas in our study Re_{d_0} was kept constant, in [2] U_j was kept constant while A was made to vary keeping the exit area of the nozzle the same. Also in [2] d_0 is used to nondimensionalize x .

The axisymmetric region of the jet is characterized by a decay of $(U_c/U_j)^2$ of slope -2 . This occurs for all jets tested at large x/θ . The proper scaling parameters for x in this region of the jet is the diameter of a circular nozzle of the same exit area as the rectangular nozzle. In fact, if we plot $(U_c/U_j)^2$ vs $\bar{x} = x_j \sqrt{(4A_e/\pi)}$ where A_e is the nozzle effective momentum area:

$$A_e = \int_{-x}^{+x} \int_{-y}^{+y} \left(\frac{U}{U_j}\right)^2 dx dy$$

The jet width. The jet width is defined by the two parameters l and d , where l is twice the distance from the centerline to the point on the z axis where $U = (U_c/2)$, and d a similarly defined distance in the y direction.

Detailed traverses of the flow fields produced results presented in Fig. 2. For the nozzles having sharp edges l and d are very similar to the results of Trentacoste and Sforza: l decreases initially while d increases so that eventually d outgrows l . Further downstream l and d grow at appreciably the same rate and the two curves seem to tend to each other. A similar variation has been observed in the wake of an ellipse by Kuo and Baldwin [9]; they noted that at some distance from the ellipse, the wake cross section is an ellipse with major axis normal to the normal axis of the wake producing ellipse. This effect is not as noticeable in the jet out of the long channel, l remains roughly constant up to a certain distance, it then starts to grow at about the same rate as d .

These results are consistent with the centerline velocity decay discussed above; the jet out of the channel remains two-dimensional further downstream than the jet out of the nozzle with sharp edges.

Mean velocity profiles. The velocity profiles taken in the two planes of symmetry of the jet at different distances from the orifice are shown in Figs. 3 and 4.

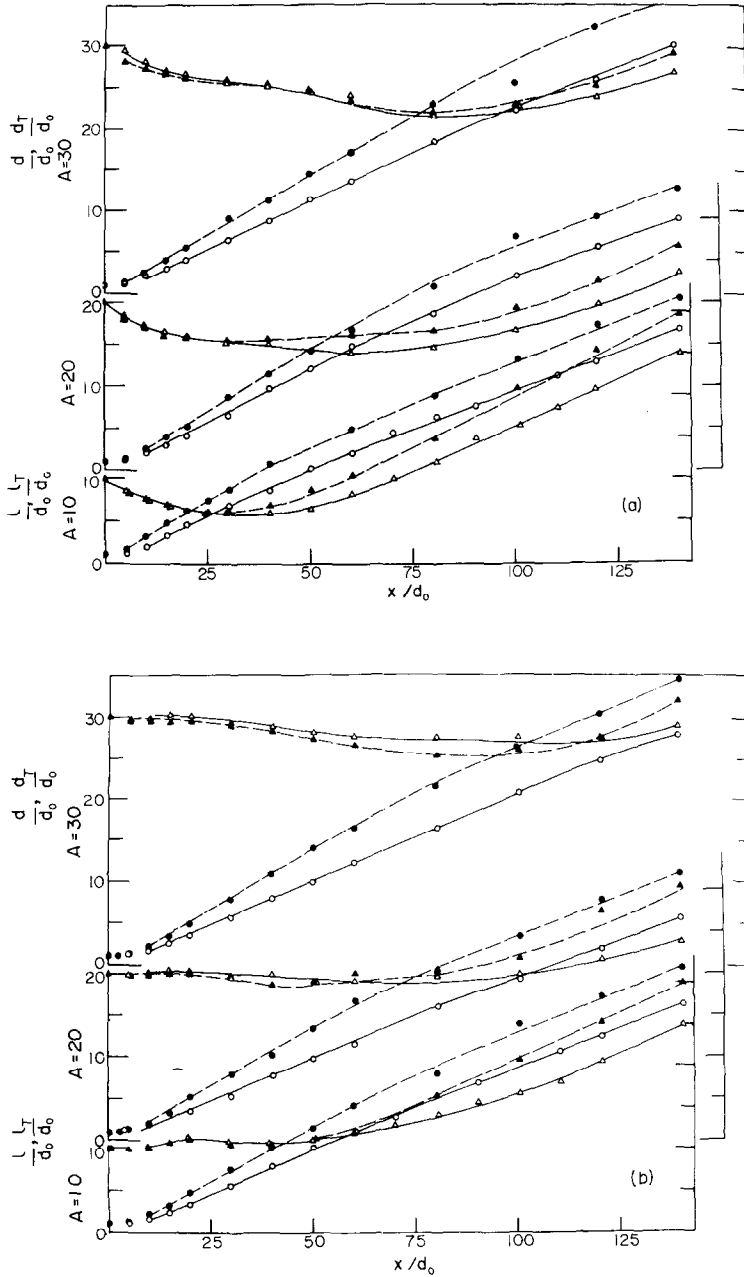


FIG. 2. Jet width. \circ , d/d_0 ; \bullet , d_T/d_0 ; \triangle , l/d_0 ; \blacktriangle , l_T/d_0 .

The velocity is nondimensionalized with respect to the centerline velocity $\bar{U} = (U/U_c)$. The y and z coordinates are nondimensionalized with respect to the distance from the hypothetical origin of the jet x' as determined from Fig. 2, $\eta = (y/x')$ and $\xi = (z/x')$.

In general $\bar{U}(\eta)$ is comparable to the results of previous two-dimensional jet measurements if the half-velocity points are made to coincide. The jet spreading coefficients d/x' shown in Table 2 are found to be quite close to previously published data, except for the flow out of the nozzle with sharp edges where the jet spreading is quite a bit faster.

The profiles $\bar{U}(\xi)$ for $A = 10$ both nozzle types develop, soon after the nozzle exit, the so-called "saddle

back" shapes which were first noted by Van Der Hegge Zijnen [4]. This shape is however more pronounced for the jet out of the sharp orifice. The data for the two other aspect ratios, not shown here, gives qualitatively very similar results. At larger distances downstream $\bar{U}(\xi)$ starts resembling $\bar{U}(\eta)$ as the jet tends to axisymmetry.

4.2. The mean temperature field

Similar to the velocity, the temperature field is described in terms of the temperature decay along the centerline, the jet width and the temperature profiles in the two planes of symmetry of the jet.

Centerline temperature decay. This is shown on Fig. 1.

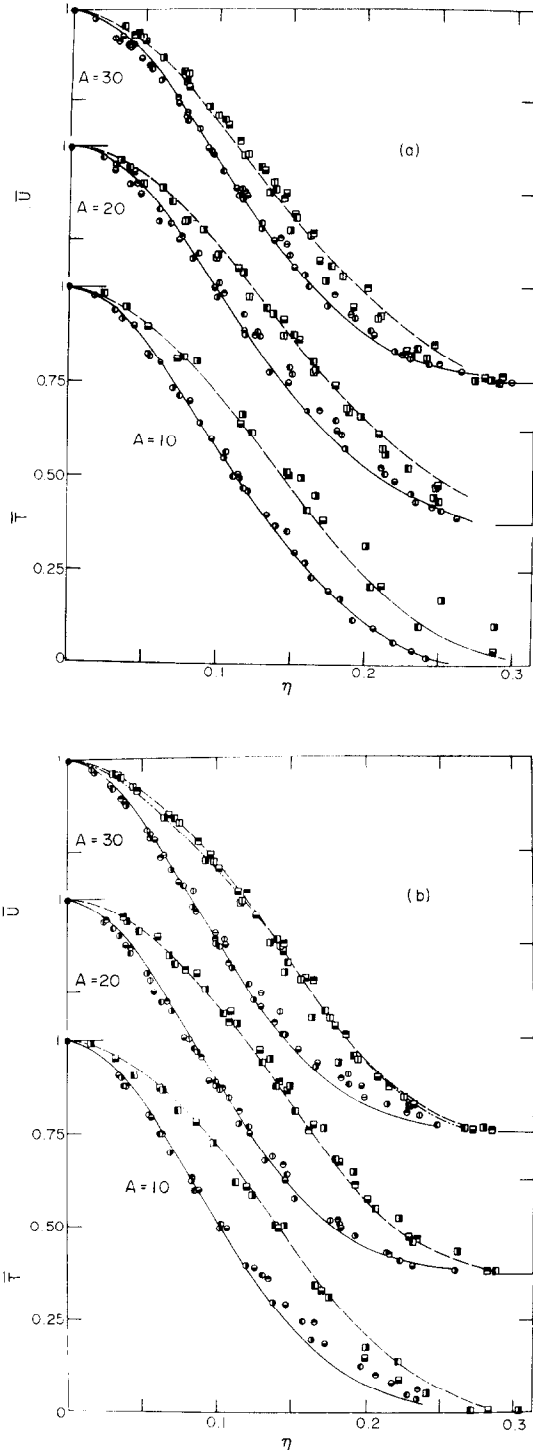


FIG. 3. Velocity and temperature profiles along y : (a) nozzle type I; (b) nozzle type II. \circ and \square , $U(\eta)$ and $\bar{T}(\eta)$ for $x/d_0 = 10$; \bullet , \blacksquare , $x/d_0 = 20$; \ominus , \blacksquare , $x/d_0 = 30$; \odot , \blacksquare , $x/d_0 = 40$; \bullet , \blacksquare , $x/d_0 = 50$; \oplus , \blacksquare , $x/d_0 = 60$. — — — — — experimental curve fit [4].

The distance downstream of the jet is non-dimensionalized by dividing it by θ_T where:

$$\theta_T = \int_{-\infty}^{+\infty} \frac{UT}{U_j T_j} dy$$

Table 2. The jet width

Nozzle type I	d	d_l
	x	x
$A = 10$	0.113	0.150
$A = 20$	0.125	0.150
$A = 30$	0.118	0.145
Nozzle type II		
$A = 10$	0.104	0.138
$A = 20$	0.103	0.143
$A = 30$	0.104	0.145

θ_T is the total heat flux across the jet to within ρC_p . It is equal to d_0 if one has a uniform temperature and velocity distribution at the jet mouth which is not the case for the velocity in both nozzle geometries tested. For reasons explained earlier, the value of θ_T was deduced from velocity and temperature profiles measured at $(x/d_0) > 1.5$.

The centerline temperature decay is found to behave the same way as the velocity: close to the jet exit there is a "potential" core region where $(T/T_j) = 1$, followed by the two-dimensional region $(T/T_j)^2 \propto (\theta_T/x)$, then a final axisymmetric region extending to infinity where $(T/T_j) \propto (\theta_T/x)$. The spread of temperature being faster than that of momentum, the potential core for temperature distribution is shorter than that for the velocity. In the two-dimensional region of the jet the data is well represented by equation (6), the values of the constants K_2 obtained are shown in Table 1. If one uses

$$A_e T = \int_{-\infty}^{+\infty} \int_{-\infty}^{+\infty} \frac{UT}{U_j T_j} dx dy$$

as the scaling parameter for x in the axisymmetric region of the jet, it is found that the data for the different aspect ratios is well represented by equation (7) where L_2 is practically independent of the aspect ratio. Values of L_2 are listed in Table 1.

The jet width. Two parameters d_T and l_T determined in the same way than d and l , but with respect to the temperature distribution, define the jet widths in the planes of symmetry of the jet. These parameters are shown in Fig. 2. In the two-dimensional region of the jet d_T increases linearly with x at a faster rate than d . On the other hand l_T remains quite close to l and they both vary as described earlier. In the region of transition to axisymmetry and further downstream l_T becomes larger than l and eventually we get $(l_T/l) \simeq (d_T/d)$.

Mean temperature profiles. The temperature profiles across the jet are shown in Figs. 3 and 4 where $\bar{T} = (T/T_c)$. A curve through the mean values of the temperature distributions as measured by Van Der Hegge Zijnen and given by the empirical curve-fit equation:

$$\bar{T} = (1 + 30\eta^2 + 2200\eta^4 - 30000\eta^6)e^{-7.5\eta^2}$$

is included on Fig. 3 for comparison; quite a good agreement is observed between his results and ours.

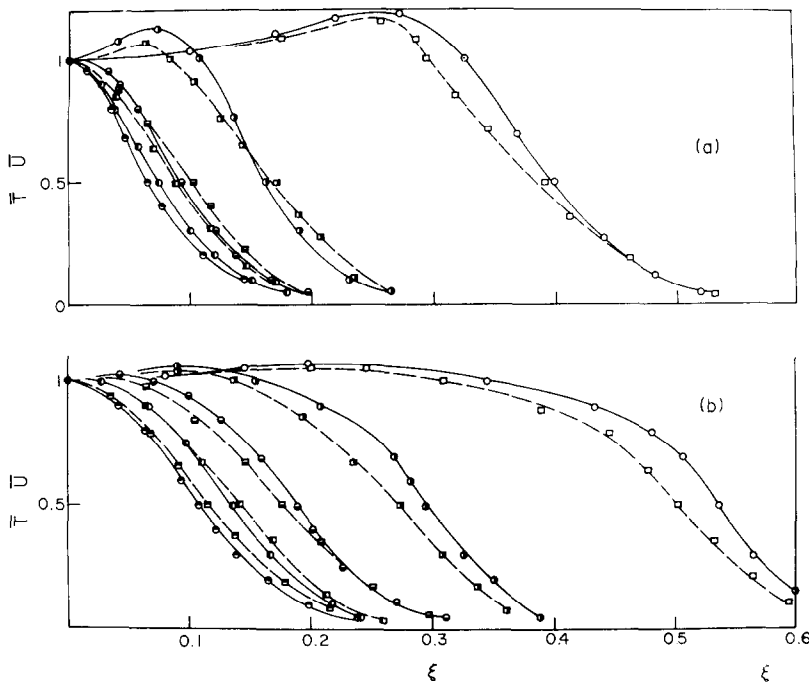


FIG. 4. Velocity and temperature profiles along z : (a) nozzle type I; (b) nozzle type II; (for legend refer to Fig. 3).

$\bar{T}(\xi)$ for $A = 10$ is shown in Fig. 4 where it may be observed that, as for $\bar{U}(\xi)$, at some distance from the slit the profile assumes a "saddle back" shape. At larger distances downstream, and as the jet becomes roughly axisymmetric, $\bar{T}(\xi)$ tends to have a shape similar to $\bar{T}(\eta)$. The data for the other two aspect ratios not shown here, behave in a qualitatively similar way.

5. DISCUSSION OF EXPERIMENTAL RESULTS

The centerline velocity and temperature decays in the two-dimensional region of the jet are well represented by equation (6) where x is nondimensionalized by dividing it by θ and θ_T respectively. The constants K_1 and K_2 obtained by fitting equation (6) to the experimental points are shown in Table 1. The results of Trentacoste and Sforza [2], who found that for A varying from 10 to 40 the exponent of \bar{x} varies from -0.64 to -1 were not confirmed in the present study. In fact, in a related study to be published later, it has been found that, for some nozzle geometries and Reynolds numbers, the nozzle geometry may influence the flow downstream to such an extent that, for small A , no parts of the flow will have a centerline velocity decay as in (6). In other words, no station of the flow is removed far enough from nozzle influence at one end and three dimensionality effects at the other in order for the centerline velocity to reach the self-preserved form of equation (6). This may explain the anomalous variation of "n" noted in [2]. Furthermore, the fact that the mean velocity field and the mean temperature field are well represented by equation (6) does not necessarily imply that the jet has reached a fully self-preserved

structure before three dimensional effects start to be felt. It is well known that self-preservation is accomplished by stages starting with the mean flow, then the turbulent stresses, the turbulent transport terms etc. . . .

In the three-dimensional region of the jet the data points are fairly well correlated by equations (7). The constants obtained by fitting the data to these equations are found in Table 1. L_1 and L_2 seem to depend little on A and are quite close to similarly defined constants for the axisymmetric jet. It is therefore, possible to deduce that both the velocity and temperature fields in the far flow of a slot jet are similar to that of a circular jet having the same momentum and heat flux.

Assuming $\theta = \theta_T = d_0$ and $A_e = A_{eT} = l_0 d_0$, an assumption which is approximately true, it can be deduced that the transition from two-dimensional to axisymmetric flow occurs at a distance from the jet mouth given by:

$$\left[\frac{x}{d_0} \right]^* = \frac{L_1^2 4A}{K_1 \pi} \tag{8}$$

for the centerline velocity, and at:

$$\left[\frac{x}{d_0} \right]^* = \frac{L_2^2 4A}{K_2 \pi} \tag{9}$$

for the centerline temperature decay. These results should be used only as a rough indication of the location of transition. Equation (8) predicts a location for the transition about 20% larger than the results of Trentacoste and Sforza [2] who find:

$$\left[\frac{x}{d_0} \right]^* \approx 5A.$$

Equations (8) and (9) are more valid for jets out of long channels. For the nozzles with sharp edges, transition occurs over a distance of the same order as the length of the two-dimensional region itself and one cannot properly speak of a transition point.

The mechanism of transition from two-dimensional to axisymmetry is not yet fully understood. It can almost certainly be said that it is not due to a simple redistribution of momentum, heat or other parameters, by turbulent stresses and other turbulent transport terms. There are good reasons to believe that vortex rings generated at the orifice play an important role in this transition. Such vortex rings have already been mentioned by Van Der Hegge Zijnen [4] in order to explain the "saddle back" shapes of the $\bar{U}(\xi)$ profiles. More evidence about the turbulent structure of the flow field is necessary in order to fully understand the mechanism of transition.

The jet width in the ξ direction is roughly the same for both the temperature and velocity distributions as may be seen from Fig. 2. This suggests the idea that the diffusion and jet growth in the ξ direction, does not have the same mechanism as one expects in turbulent diffusion, for then, T would have diffused much faster than U as in the case along the η direction. At larger distances downstream, the diffusion and jet growth tends to become the same along ξ and η .

Acknowledgement—The author wishes to express his deep gratitude to the American University of Beirut for its support in this project.

REFERENCES

1. P. M. Sforza, M. H. Steiger and N. Trentacoste, Studies on three-dimensional viscous jets, *A.I.A.A. Jl* **4** (5), 800 (1966).
2. N. Trentacoste and P. M. Sforza, Further experimental results for three-dimensional free jets, *A.I.A.A. Jl* **5** (5), 885 (1967).
3. P. M. Sforza, A quasi-axisymmetric approximation for turbulent three-dimensional jets and wakes, *A.I.A.A. Jl* **7** (7), 1380 (1969).
4. B. G. van der Hegge Zijnen, Measurements of the velocity distribution in a plane turbulent jet of air, *Appl. Scient. Res.* **A7**, 256 (1958); Measurements of the distribution of heat and matter in a plane turbulent jet of air, *Appl. Scient. Res.* **A7**, 277 (1958).
5. L. J. S. Bradbury, The structure of the self-preserving turbulent plane jet, *J. Fluid Mech.* **23** (1), 31 (1965).
6. G. Heskestad, Hot wire measurements in a plane turbulent jet, *J. Appl. Mech.* **85E**, 721 (1965).
7. B. El-assad, Flow studies and turbulence measurements in a prototype low-speed blow-down wind tunnel, M. S. Thesis, American University of Beirut, Department of Mechanical Engineering (1973).
8. A. A. Townsend, The structure of turbulent shear flow. Cambridge University Press, London (1965).
9. Y. H. Kuo and L. V. Baldwin, The formation of elliptical wakes, *J. Fluid Mech.* **27** part 2, p. 353 (1967).
10. M. J. Albertson *et al.* Diffusion of submerged jets, *Proc. Am. Soc. Chem. Engrs.*, Vol. 74, p. 1571 (1948).
11. W. Forstall and E. W. Gaylord, Momentum and mass transfer in a submerged water jet, *J. Appl. Mech.* **22**, 161 (1955).
12. J. O. Hinze and B. G. van der Hegge Zijnen, Transfer of heat and matter in the turbulent mixing zone of an axially symmetric jet, *Appl. Scient. Res.* **A1**, 435 (1949).

CHAMPS DE VITESSE ET DE TEMPERATURE DANS LES JETS RECTANGULAIRES

Résumé—On a mesuré les vitesses moyennes et températures moyennes à l'aide d'un anémomètre à fil chaud dans des jets rectangulaires présentant différents rapports de dimensions et plusieurs géométries de buse. L'écart de température dans le jet étant faible, la température a pu être traitée comme un scalaire passif. On peut distinguer dans les champs de vitesse et de température, trois régions distinctes respectivement désignées par: le noyau potentiel, la région bidimensionnelle et la région axisymétrique. Ces régions relatives aux distributions de vitesse d'une part et de température d'autre part, ne coïncident pas. L'étendue de chacune d'entre elles dépend du rapport des dimensions de l'orifice. L'écoulement dans la région bidimensionnelle ainsi que la transition vers la région axisymétrique est fortement fonction de la géométrie du bec. A de grandes distances de l'orifice, il apparaît que les champs de vitesse et de température se comportent comme dans l'écoulement issu d'un orifice circulaire d'aire égale.

DAS GESCHWINDIGKEITS- UND TEMPERATURFELD IN STRAHLEN MIT RECHTECKIGEM QUERSCHNITT

Zusammenfassung—Die mittlere Geschwindigkeit und die Temperatur von Strahlen mit rechteckigem Querschnitt wurde bei verschiedenen Seitenverhältnissen und Düsengeometrien mit Hilfe eines Hitzdrahtanemometers gemessen. Die Exzess-Temperatur im Strahl war klein, so daß die Temperatur als passiver Skalar betrachtet werden konnte. Sowohl für das Geschwindigkeits- wie für das Temperaturfeld kann das Strömungsfeld in 3 verschiedene Bereiche unterteilt werden, nämlich einen Potentialkern, einen Bereich zweidimensionaler Strömung und einen axisymmetrischen Bereich. Diese Bereiche stimmen jedoch nicht überein für das Geschwindigkeits- und das Temperaturfeld. Die Ausdehnung der einzelnen Bereiche ist abhängig vom Seitenverhältnis der Düse. Die Strömung im zweidimensionalen Bereich und der Übergang zur Axialsymmetrie können als eindeutige Funktionen der Düsengeometrie angegeben werden. Bei großen Entfernungen von der Düse stimmen die Geschwindigkeits- und Temperaturfelder mit denen eines, aus einer kreisförmigen Düse ausströmenden Strahles überein.

ПОЛЯ СКОРОСТИ И ТЕМПЕРАТУРЫ СТРУЙ ПРЯМОУГОЛЬНОГО СЕЧЕНИЯ

Аннотация — С помощью термоанемометра измерены средняя скорость и температура прямоугольных струй при различных отношениях сторон и геометриях сопла. Температура струи была мало отличной от температуры окружающей среды, так чтобы ее можно было рассматривать как пассивный скаляр. Найдено, что как скоростное, так и термическое поля потока делятся на три четкие области, а именно потенциальное ядро, двумерную область и осесимметричную область, отличимые по распределению скорости и температуры. Величина каждой из этих областей зависит от отношения сторон сопла. Течение в двумерной области, как и в области перехода к асимметрии, сильно зависят от геометрии сопла. Найдено, что на больших расстояниях от выхода из сопла поля скорости и температуры аналогичны полям при истечении из круглого сопла той же площади.